Structural, Electronic, and Magnetic Properties of Fe_3C_2 Cluster

Mei-Yu Sun, Chuan-Lu Yang,* Mei-Shan Wang, Yu-Bing Gong, Ying-Tao Zhu, and Wei Liu

College of Physics and Electronic Engineering, Ludong University, Yantai 264025, People's Republic of China

Received: December 29, 2007; Revised Manuscript Received: February 23, 2008

On the basis of density-functional theory and all-electron numerical basis set, 20 stable isomers of Fe_3C_2 cluster are found through optimization calculations and frequency analysis from 108 initial structures. A nonplanar C_s structure with nonet spin multiplicity and 482.978 kcal/mol of binding energy is found as the candidate of global minimum geometry of Fe_3C_2 cluster. The binding energies, the energy gaps between the highest occupied molecular orbital and the lowest unoccupied molecular orbital, and the magnetic moments of all the isomers are reported. The relationship between the molecular properties and geometrical structures is also investigated.

1. Introduction

The Fe-based nanoparticles are of great interest because they play an essential role in modern materials science. A large number of experimental and theoretical investigations of bare iron clusters[1–19] have been carried out. For example, the polarizabilities of Fe_n ($n \leq 4$) clusters have been investigated by Calaminici.[20] Recent investigation shows that iron clusters can act as a catalyst in the production of single-walled carbon nanotubes (SWNT).[21] Some studies on the Fe-based nanoparticles including Fe with O[22] and Fe with C have also been reported. The bonding of methane with magnetic Fe_4 clusters have been investigated by Castro.[23] More studies devoted to the FeC_n or Fe_nC clusters can be found in the literature. Gutsev and Bauschlicher[24] have computed the electronic and geometrical structures of the ground and excited states of Fe_nC, Fe_nC^-, and Fe_nC^+ ($n = 1-6$) clusters using density functional theory (DFT). Nash et al.[25] have calculated the equilibrium geometries, total energies, and electronic structures of FeC_n ($n \leq 3$) clusters using three levels of theory. They found that the density functional theory is accurate in explaining the experiment and can be used to study larger clusters of FeC_n reliably. The FeC_2 molecule in its different geometric conformations and electronic states has been studied using the DFT (B3LYP) and CASSCF/CASPT2 methods.[26] It is shown that the cyclic (C_{2v}) structure of FeC_2 molecule is more stable than the linear ($C_{\infty v}$) structure. Sosa et al.[27] have computed triplet and quintet states of Fe_5C, neither of which is the ground-state of the cluster. Krause et al.[28] have computed $Fe_{21}C$ and $Fe_{27}C$ at the assumed geometries to simulate two nonequivalent sites in bulk Fe_4C. Noya et al. have reported ab initio calculations of the structures, binding energies, and spin multiplicities of the clusters Fe_2, C_2, FeC_n ($n = 1-4$), and Fe_2C_n ($n = 1-3$) using DFT method.[29] They pointed out that all the dimetallic carbide clusters are predicted to have cyclic planar geometries that are stabilized by transannular bonds.[29] They also found that the pentagonal geometries of Fe_2C_3 with transannular Fe−Fe and Fe−C bonds include a FeC_2 unit that is almost identical to free FeC_2. Subsequently, they expanded their investigation to Fe_2C_4 and found the ground-state structure is also a planar ring that feature nonadjacent Fe atoms.[30] Fe_nC_{12} ($n = 2-8$) clusters were experimentally studied by Pilgrim and Duncan,[31] and DFT investigations of Fe_nC_{12} ($n = 2-8$) clusters were carried out by Harris and Dance[32] very recently. On the basis of DFT calculations, Ryzhkov and co-workers have searched stable structures of Fe_2C, FeC_2, Fe_3C, FeC_3, and Fe_2C_2 using "binomial" scheme[33] to build initial geometries. They found that the most stable planar structures for FeC_3 and Fe_2C_2 are favored over the three-dimensional isomers, whereas for Fe_3C the pyramidal configuration appeared to be the ground state. However, the investigations of Fe_nC_m clusters are still inadequate, limiting the understanding of their roles in various chemical and physical processes.

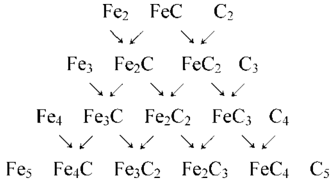

Figure 1. The scheme of building initial structures for search of the stable structures for Fe_mC_n [from ref 33].

Stimulated by the previous investigations of Fe_2C_2 and Fe_3C clusters by Ryzhkov et al.[33] and Fe_2C_3 clusters by Noya et al.,[29,30] we present an extended investigation of the Fe_3C_2 cluster. In the present work, we seek the stable isomers of the Fe_3C_2 cluster. The binding energies (BE), vibrational frequencies, energy gaps between highest occupied molecular orbital (HOMO) and lowest unoccupied molecular orbital (LUMO), and the magnetic moments of the stable structures are calculated and analyzed. It is expected that the present results can provide a basis for understanding the molecular properties of the various isomers of Fe_3C_2 cluster.

2. Computational Details

We search for the stable geometries of Fe_3C_2 cluster still following the binomial scheme[33] [see Figure 1]. In the scheme, the Fe or C atom is made to approach the initial dimers Fe_2, FeC, and C_2 from all possible directions, which will result in some stable configurations of Fe_2C, FeC_2, Fe_3, and C_3. Then these stable structures are served as basic units for generating the initial structures of tetraatomic clusters and so on. We extend the scheme to the Fe_3C_2 cluster containing five atoms in the

---

* Author to whom correspondence should be addressed. E-mail: yangchuanlu@263.net

10.1021/jp7121592 CCC: $40.75

TABLE 1: the Calculation Results for Fe_2C_2 and Fe_3C Clusters, Including Those of Ryzhkov et al

	symmetry	binding energy (kcal/mol)	
isomers	present	present	Ryzhkov et al.[32]
Fe_2C_2-1	C_s	397.005	397
Fe_2C_2-2	D_{2h}	391.182	391
Fe_2C_2-3	$D_{\infty h}$	389.034	389
Fe_2C_2-4	C_{2v}	386.760	388
Fe_2C_2-5	D_{2h}	381.544	383
Fe_2C_2-6	C_{2v}	356.381	357
Fe_2C_2-7	$C_{\infty v}$	359.732	357
Fe_2C_2-8	C_1	340.749	341
Fe_2C_2-9	C_s	338.618	340
Fe_2C_2-10	C_s	333.561	334
Fe_2C_2-11	C_s	332.408	333
Fe_2C_2-12	$D_{\infty h}$	306.520	304
Fe_3C-1	C_{3v}	322.644	323
Fe_3C-2	C_{2v}	319.703	320
Fe_3C-3	C_{2v}	314.669	315
Fe_3C-4	$C_{\infty v}$	289.006	289

present paper. According to the scheme, there are two ways to build initial structures for searching the stable configurations of Fe_3C_2. The first one is to add a Fe atom to the tetraatomic Fe_2C_2 cluster, and the other is to add a C atom to the Fe_3C cluster. Hereinafter, they are represented by “a” and “b”, respectively.

Because the number of the possible initial structures of Fe_3C_2 is large, the work to search the stable geometries for Fe_3C_2 cluster cannot be fulfilled if there is no efficient computational method. As Ryzhkov et al.[33] mentioned in their article, the DFT-based $DMol^3$ method[34] is very efficient and may serve our purpose, because it can search for optimum atomic positions based on the total energy gradient calculation. All the calculations for geometry optimization of Fe_3C_2 isomers are performed using the spin-polarized DFT calculations with the generalized gradient approximation (GGA) in “PW91” form.[35,36] The molecular DFT $DMOL^3$ package is employed in which double numerical plus d-functions (DND) are chosen to describe the electronic wave functions. It is a set of default basis set in the package, providing reasonable accuracy for modest computational cost.

At first, we recalculate the 16 stable structures of Fe_2C_2 and Fe_3C reported by Ryzhkov et al.[33] to confirm the convergence standard and parameters of the numerical calculations used in the present work. Our results and those of Ryzhkov et al.[33] are collected in Table 1. In our calculations, optimization is performed by the convergence settings of 1.0×10^{-5} Hartree for the energy, 5.0×10^{-4} Hartree/Bohr for the maximum force and 0.002 Å for the maximum displacement. The global orbital cutoff is 6.0 Å, which is better than the “fine” standard in $DMol^3$. The smearing gap 0.005 is used to facilitate the convergence of the SCF iterations. Table 1 shows that our binding energies are in accord with those of Ryzhkov et al.[33] although small differences exist in some structures. The above parameters are employed in all the following calculations to search the stable geometries. However, many optimization structures are found within a small energy range, which is a common character for the systems containing transition metal atoms. To obtain a more precise ordering of the optimization structures, produce better relaxation of the Fe−Fe, Fe−C, and C−C bonds, and yield much better geometries, we recalculate all the optimization structures using much tighter convergence criteria (10^{-8} thresholds for the total energy and 10^{-5} for the forces).

It should be noted that the twelfth structure ($D_{\infty h}$) reported by Ryzhkov et al.[33] is not a stable geometry in our calculation although the much tighter convergence criteria is employed. There are four imaginary vibrational frequencies in the twelfth structure although our BE is 306 kcal/mole, which is close to their 304 kcal/mol.[33] However, we still use it to construct the Fe_3C_2 initial structures to avoid missing the possible stable isomers from this way.

3. Results and Discussions

3.1. Stable Geometries and Binding Energies. Following the two ways (“a” and “b”) of building initial structures in Section 2, the Fe or C atom is added to the pre-existing Fe_2C_2 and Fe_3C clusters from many spatial directions, and we obtain 108 initial geometries in total, including 83 from “a” way and 25 from “b”.

The initial geometries are subjected to geometrical optimization and frequency analysis, leading to 50 stable structures, including 39 stable structures for the initial structures from “a” and 11 stable structures from “b”. All the optimization structures are shown in Figure 2. To distinguish the additional Fe or C atom from the others more clearly, we delete the bonds connecting between the added atom and the other atoms in the figures, that is, the separate Fe atom is the added atom. As shown in Figure 2, the geometries include 31 planar and 19 three-dimensional structures, and no linear structure has been found.

However, checking the geometries carefully, we find that the BEs and bond lengths of some structures have only small differences. The similar structures look like the same stable structure although their geometries belong to different point groups because they are optimized from initial structures with different symmetries. We guess that the similar stable structures may be the same geometry actually, and the small differences result from the errors of the same geometry calculated with the molecular orbital with different symmetries. To confirm the idea, we repeat optimizations and frequency calculations with much tighter convergence criteria using all the 50 structures as initial structures. This time, the same symmetry is used for the similar structures by a loose standard to determine the symmetries of the isomers. For example, C_s symmetry is used in the recalculations for the similar geometries (the isomer numbers are 14, 15, 16, 17, 18, 20, and 21). The new calculation results show that the differences of their BEs are smaller than 1.0 kcal/mol (chemical accuracy) although some of the bond lengths are different to some extent. We will treat them as the same structure in following discussions. Moreover, six other groups of the structures are the similar cases. The isomer numbers of the six groups are 23/24/25, 31/32/33, 37/38/39, 40/41, 42/43/44, and 49/50, respectively. However, we have also noted that the BE difference between isomer 12 and isomer 21 is only 0.9 kcal/mol, and the biggest difference of the bond lengths is 0.053 Å in the first calculations. To our surprise, the reoptimizations show that the difference of their BEs is enlarged to 7.0 kcal/mol, and the biggest difference of bond lengths is 0.327 Å. They are obviously not the same but two completely different stable structures. It is also found that 7 structures of the 50 geometries, that is, isomers 4, 5, 9, 10, 22, 45, and 48 are unstable geometries with imaginary frequencies in the recalculations. Besides, the recalculations of other 7 structures cannot reach the new tight convergence criteria in the SCF iterations or optimization. The different calculation results in the recalculations may be understood in that the different initial molecular orbitals (including the representations and occupations) of the SCF calculations have been used. As explained before, the twelfth structure reported by Ryzhkov et al.[33] is not stable in our calculation, and we also have not obtained any stable structures of Fe_3C_2 from the initial structures by adding a Fe atom to it.

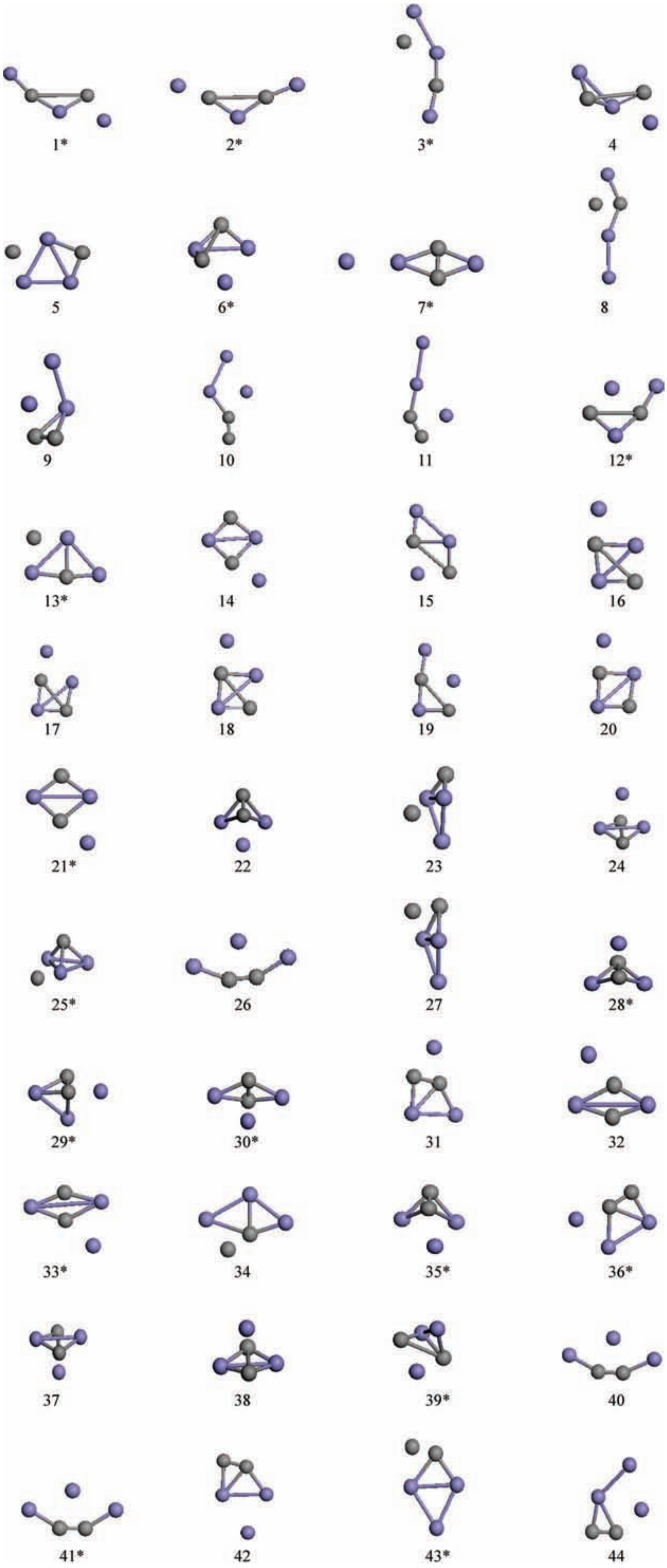
1*
2*
3*
4
5
6*
7*
8
9
10
11
12*
13*
14
15
16
17
18
19
20
21*
22
23
24
25*
26
27
28*
29*
30*
31
32
33*
34
35*
36*
37
38
39*
40
41*
42
43*
44

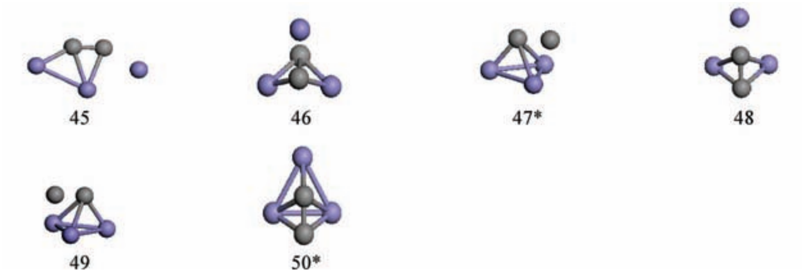

Figure 2. The 50 optimized geometries from the 108 initial structures of Fe_3C_2 cluster. They are arranged in order of increasing absolute values of BEs. Among them, only 20 structures turn out to be stable after recalculations. The asterisk represents that the corresponding structure is stable. The carbon atoms are given in gray, and iron atoms are shown in purple.

TABLE 2: The BEs, Bond Lengths and HLEGS of All the 20 Stable Isomers of Fe_3C_2 Cluster

isomer number	symmetry	BEs (kcal/mol)	C−C bond (Å)	Fe−Fe bond (Å) min	Fe−Fe bond (Å) max	Fe−C bond (Å) min	Fe−C bond (Å) max	HLEG (eV)
1	C_s	420.829	3.013	2.431	5.744	1.669	4.374	0.587
2	C_{2v}	424.903	2.780	3.361	5.803	1.648	4.341	0.430
3	C_s	425.392	2.876	2.504	5.681	1.680	4.218	0.500
6	C_1	448.689	2.805	2.314	2.611	1.713	3.063	0.719
7	C_{2v}	449.910	1.392	2.333	5.813	1.864	4.143	0.404
12	C_s	456.587	2.611	2.324	3.516	1.707	3.839	0.363
13	C_s	460.499	2.594	2.464	3.503	1.710	3.864	0.064
21	C_s	463.551	2.284	2.344	3.533	1.716	3.636	0.700
25	C_s	465.435	2.401	2.356	2.528	1.740	3.078	0.574
28	D_{3h}	465.679	2.310	2.365	2.365	1.789	1.789	0.741
29	C_1	467.755	1.420	2.240	3.482	1.869	2.071	0.468
30	C_{2v}	469.214	1.424	2.310	3.490	1.924	2.028	0.515
33	C_s	471.412	1.405	2.308	3.630	1.826	2.984	0.547
35	C_1	472.830	1.362	2.442	2.595	1.880	3.072	0.819
36	C_s	473.686	1.325	2.197	3.707	1.780	3.111	0.459
39	C_{2v}	476.009	2.298	2.300	2.644	1.768	2.005	1.048
41	C_{2v}	478.745	1.305	2.389	4.365	1.798	2.988	0.699
43	C_s	479.994	1.296	2.331	2.457	1.878	4.092	0.628
47	C_s	482.859	1.348	2.273	2.309	1.843	2.890	0.653
50	C_s	482.978	1.346	2.267	2.307	1.846	2.887	0.586

Finally, we obtain 20 different stable isomers for Fe_3C_2 in total. Their geometrical properties in Figure 2 are updated according to the recalculation results. Their bond lengths and BEs are collected in Table 2. The largest bond length of C−C is 3.013 Å of isomer 1, and the shortest is 1.296 Å of isomer 43. There are 6 values of Fe−C in every isomer. However, we only list the minima and the maxima in the Table 2. The minima for the all isomers range from 1.648 to 1.924 Å and the maxima 1.789 to 4.374 Å. There are three values of Fe−Fe in every isomer. We still list the minima and the maxima for the isomers.

In Figure 3, we plot the BEs and the bond lengths of all the isomers to show the relationship between the BEs and the structures of the isomers for Fe_3C_2. From the figure, we find that the larger BE clusters generally have more compact geometries. The Fe−Fe maximum bond length of each isomer affects the BEs obviously, for example, isomers 1, 2, and 3 have obviously smaller BEs than those of the others, whereas their Fe−Fe maxima are also obviously larger. It should be noted that the bond length of C−C also plays an important role for the BEs. In particular, among structures 36, 41, 43, 47, 50, and 28, the structure 28 looks more compact than the others but has a smaller BE; however, it is not true because the C−C bond length of the structure 28 (2.310 Å) is much larger than that of the others. Therefore the structure 28 should be less compact although its other bond lengths are slightly smaller. From Figure 3 and Table 2, we can conclude that isomer 50 with the largest BE of 482.978 kcal/mol can be regarded as the candidate for the global minimum of Fe_3C_2 cluster, and it means that the most stable structure energetically is also the most compact structure. Ryzhkov et al.[33] have concluded that for 3- and 4-atom nanoparticles of Fe_nC_m, linear structures cannot be the ground state even for the triatomic species, and highly symmetric structures for the cluster do not lead to the most stable geometry in general. The present investigation shows that for the Fe_3C_2 cluster the most stable structure is in the C_s symmetry but not in D_{3h}, and no linear structure is found to be stable, which is in agreement with the conclusion of Ryzhkov et al. As Fe_2C_n (n = 1−3) clusters reported in the literature,[29,30] Fe_3C_2 cluster also has planar structures. Seven stable cyclic planar geometries (isomer 12, 13, 21, 33, 36, 41, and 43) are found at the present calculational level.

3.2. HOMO−LUMO Energy Gaps. The electronic properties of Fe_3C_2 cluster can also be investigated through examining HOMO−LUMO energy gap (HLEG). The HLEGs for the all 20 stable structures are collected in Table 2. We can find from the table that the HLEGs for the isomers are obviously different, and the HLEGs range from 0.064 to 1.048 eV. It implies that the isomers of Fe_3C_2 cluster have various abilities to control electrons and can be used as different objectives for various chemical reactions. The one with the largest 1.048 eV of HLEG is isomer 39. As shown in Figure 4, for isomer 39, the HOMO is located partly on the C atom, and the LUMOs are almost completely located on the three Fe atoms. For isomer 13 with the smallest HLEG of 0.064 eV, its LUMO is located partly on C atom although the HOMO still is mainly on the Fe atoms. We also examine the HOMO and LUMO for all other isomers and find that the HOMOs for all isomers mainly locate on Fe atoms, while the LUMOs locate on a small part of the orbital

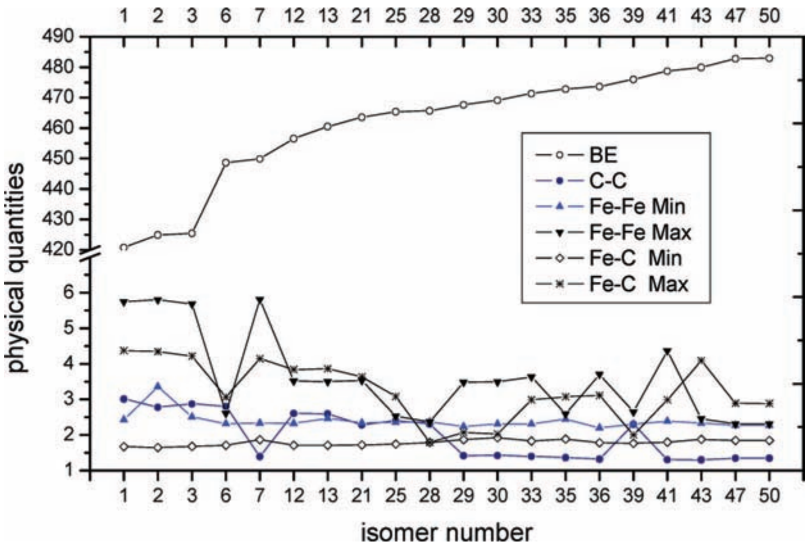

Figure 3. Binding energies and bond lengths of the 20 stable geometries of Fe_3C_2 cluster. Only the maxima and minima values for the Fe−Fe and Fe−C bonds of each isomer are plotted although there are 3 bonds for Fe−Fe and 6 bonds for Fe−C. Here, the *x*-coordinate represents the numbers of the stable isomers.

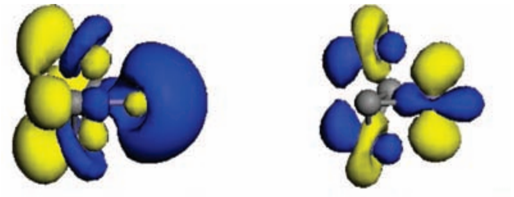
HOMO of isomer 39 LUMO of isomer 39

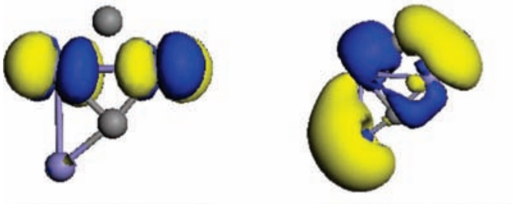
HOMO of isomer 13 LUMO of isomer 13

Figure 4. The isodensity surfaces for the HOMO and LUMO of isomer 39 and isomer 13 of Fe_3C_2 cluster. Isomer 39 is the one with the largest HLEG while isomer 13 is the one with the smallest HLEG. The carbon atoms are given in gray, and iron atoms in purple.

on C atoms; for some isomers the C component is obvious, but for the others it is too small to display in the picture. Obviously the chemical stability is dependent on the Fe atom in the isomers.

The HOMO and LUMO molecular orbital in the most stable structure (structure 50) correspond to spin down A′ and up A′ irreducible representations of the C_s point group, respectively. The HOMO contains 67.75% of the Fe 3d atomic orbital, with admixtures of Fe 4s (10.72%) and C 2p (6.50%) character, and for the LUMO the delocalized character is very obvious. The Fe 3d atomic orbital decreases to 29.76% with admixtures of Fe 4s (18.85%), Fe 4p (13.88%), C 2p (18.13%), and C 2s (10.88%) character. While for the least stable isomer (isomer 1), the HOMO and LUMO correspond to spin up orbital of A′ and A″ symmetries, respectively. The HOMO contains 61.53% 3d contributions from all Fe atoms, but the LUMO contains 89.04% Fe 3d. Generally, the HOMO and LUMO of Fe_3C_2 isomers are more delocalized than the Fe_2C isomer but similar components as the Fe_3C isomers.[35] We also noted the HLEG of the most stable geometry (structure 50) energetically is 0.586 eV and is not the one having the largest HLEG of 1.048 eV.

3.3. Magnetic Moment. On the basis of the optimized stable geometries, the magnetic properties of the 20 Fe_3C_2 isomers are investigated and the results are presented in Table 3. We also determine the corresponding spin states of the isomers by analyzing the orbital occupations. This determination is very important, because systems including transition metal Fe offer several spin states contained in a small energy range. Even if some spin states are higher energy states they may play an important role in the electronic, magnetic, or catalytic properties of the cluster.[23] From Table 3, we can find that the total magnetic moment is mainly located on the Fe atoms, and some of the local moments on C atoms are found to align antiferromagnetically with respect to that on the Fe atoms. We also find the Fe_3C_2 isomers really have various spin states, ranging from singlet to hendecatet. It is interesting to find that the local moments on one Fe atom align antiferromagnetically with respect to that on the other two Fe atoms in 7 isomers, which results in the total magnetic moment smaller than 4 μ_B, while the others are all about or larger than 6 μ_B. The one with the largest magnetic moment is isomer 43 whose magnetic moment reaches 10.01 μ_B, which is close to the 10.3 μ_B of the pure Fe_3

TABLE 3: Magnetic Moments and Corresponding Spin States of the 20 Stable Isomers (in μ_B)

isomer number	C	C	Fe	Fe	Fe	total	spin states
1	0.459	0.679	−2.136	−2.575	−2.481	−6.054	7
2	0.328	0.328	2.197	−2.456	−2.156	−1.759	3
3	−0.164	0.398	2.945	−2.476	−2.479	−1.776	3
6	0.395	0.465	−2.573	−1.873	−2.375	−5.961	7
7	0.128	0.128	−2.242	3.018	−3.405	−2.373	3
12	0.319	0.412	−2.430	−2.188	−2.243	−6.130	7
13	−0.189	0.220	2.283	−2.605	−2.461	−2.752	3
21	0.092	0.205	2.346	−2.431	−2.282	−2.070	3
25	−0.315	−0.400	2.932	1.941	1.941	6.104	7
28	0.000	0.000	0.000	0.000	0.000	0.000	1
29	−0.033	−0.090	2.824	2.744	2.821	8.264	9
30	−0.054	−0.050	2.771	2.771	2.789	8.223	9
33	0.009	0.024	3.236	−2.415	2.890	3.744	5
35	0.056	0.048	3.013	−2.388	3.182	3.911	5
36	−0.052	0.007	2.911	2.880	2.576	8.322	9
39	0.369	0.369	−3.019	−1.853	−1.853	−5.987	7
41	0.005	0.005	2.513	2.513	3.058	8.094	9
43	0.088	0.257	3.153	3.206	3.303	10.007	11
47	−0.016	−0.080	2.817	2.628	2.817	8.164	9
50	−0.013	−0.080	2.660	2.818	2.818	8.205	9

cluster at the same computational level. In this structure, the local magnetic moment on C atoms is not the largest (the largest local magnetic moment on C atom, existing in isomer 1, reaches 1.138 μ_B, but it aligns antiferromagnetically with respect to that on the other three Fe atoms; therefore it makes the total magnetic moment of isomer 1 decrease). For the most stable structure (isomer 50), all local magnetic moments on the three Fe atoms are smaller than those of isomer 43, and the local magnetic moment on C atoms aligns antiferromagnetically with respect to those of Fe atoms. Therefore, the total magnetic moment is 8.205 μ_B, which is obviously smaller than the largest 10.01 μ_B of isomer 43. Another particular case is that all the local magnetic moments on each atom are zero in isomer 28. It is the highest-symmetrical geometry (D_{3h}) among the 20 stable structures. By carefully examining the molecular orbital occupations of isomer 28, we find all the occupations of spin up and down always occur in pairs because the high-symmetrical point group provides enough degeneracy orbitals. Therefore, the total spin of each atom is zero.

4. Conclusions

Twenty stable geometries of Fe_3C_2 are found using spin-polarized DFT calculations with numerical basis sets DND. The stability of all clusters is confirmed by vibrational frequency analysis. It is found that the candidate of the global minimum structure is not the highest-symmetrical D_{3h} geometry but the most compact C_s nonplanar structure (isomer 50). Some interesting structures, such as isomer 28 with zero magnetic moment are found. The values of the BEs, HLEGs, and magnetic moments of the Fe_3C_2 isomers span a large range. It implies that the Fe_3C_2 cluster, which has rich and colorful geometrical structures and molecular properties, can play an important role in various adsorption processes or catalytic reactions.

Acknowledgment. This work is supported by the National Science Foundation of China under Grant NSFC-10674114.

References and Notes

(1) Rohlfing, E. A.; Cox, D. M.; Kaldor, A.; Johnson, K. H. *J. Chem. Phys.* **1984**, *81*, 3846.

(2) Yang, S.; Knickelbein, M. B. *J. Chem. Phys.* **1990**, *93*, 1533.

(3) Parks, E. K.; Klots, T. D.; Riley, S. J. *J. Chem. Phys.* **1990**, *92*, 3813.

(4) Wang, L. S.; Cheng, H. S.; Fan, J. *J. Chem. Phys.* **1995**, *102*, 9480.

(5) Wang, L. S.; Li, X.; Zhang, H. F. *Chem. Phys.* **2000**, *262*, 53.

(6) Armentrout, P. B. *Annu. Rev. Phys. Chem.* **2001**, *52*, 423.

(7) Billas, I. M. L.; Châtelain, A.; de Heer, W. A. *Science* **1994**, *265*, 1682.

(8) Cox, D. M.; Trevor, D. J.; Whetten, R. L.; Rohlfing, E. A.; Kaldor, A. *Phys. Rev. B* **1985**, *32*, 7290.

(9) Montano, P. A. *Solid State Commun.* **1980**, *35*, 53.

(10) Purdum, H.; Montano, P. A.; Shenoy, G. K.; Morrison, T. *Phys. Rev. B* **1982**, *25*, 4412.

(11) Moskowits, M.; DiLella, D. P. *J. Chem. Phys.* **1980**, *73*, 4917.

(12) Leopold, D. G.; Lineberger, W. C. *J. Chem. Phys.* **1986**, *85*, 51.

(13) Nour, E. M.; Alfaro-Franco, C.; Gingerich, K. A.; Laane, J. *J. Chem. Phys.* **1987**, *86*, 4779.

(14) Haslett, T. L.; Bosnick, K. A.; Fedrigo, S.; Moskowits, M. *J. Chem. Phys.* **1999**, *111*, 4917.

(15) Castro, M. *Int. J. Quantum Chem.* **1997**, *64*, 223.

(16) Gutsev, G. L.; Khanna, S. N.; Jena, P. *Phys. Rev. B* **2000**, *62*, 1604.

(17) Gutsev, G. L. *Phys. Rev. B* **2002**, *65*, 132417.

(18) Chrétien, S.; Salahub, D. R. *Phys. Rev. B* **2002**, *66*, 155425.

(19) Gutsev, G. L. *Chem. Phys.* **2003**, *291*, 27.

(20) Calaminici, P. *Chem. Phys. Lett.* **2004**, *387*, 253.

(21) Wongwiriyapan, W.; Katayama, M.; Ikuno, T.; Yamauchi, N.; Mizuta, T.; Murakami, T.; Shin-ichi Honda; Oura, K.; Kisoda, K.; Harima, H. *Jpn. J. Appl. Phys.* **2005**, *44*, 457.

(22) Cao, Z.; Wu, W.; Zhang, Q. *J. Mol. Struct.* **1999**, *489*, 165.

(23) Castro, M. *Chem. Phys. Lett.* **2007**, *446*, 333.

(24) Gutsev, G. L.; Bauschlicher, C. W. *Chem. Phys.* **2003**, *291*, 27.

(25) Nash, B. K.; Rao, B. K.; Jena, P. *J. Chem. Phys.* **1996**, *105*, 11020.

(26) Arbuznikov, A. V.; Hendrickx, M.; Vanquickenborne, L. G. *Chem. Phys. Lett.* **1999**, *310*, 515.

(27) Sosa, R.; Gardiol, P.; Beltrame, G. *Int. J. Quantum Chem.* **1997**, *65*, 919.

(28) Krause, J. C.; Paduani, C. *Hyperfine Interact.* **1997**, *108*, 465.

(29) Noya, E. G.; Longo, R. C.; Gallego, L. J. *J. Chem. Phys.* **2003**, *119*, 11130.

(30) Noya, E. G.; Longo, R. C.; Gallego, L. J. *J. Chem. Phys.* **2004**, *120*, 2069.

(31) Pilgrim, J. S.; Duncan, M. A. *J. Am. Chem. Soc.* **1993**, *115*, 6958.

(32) Harris, H. H.; Dance, I. G. *Polyhedron* **2007**, *26*, 250.

(33) Ryzhkov, M. V.; Ivanovskii, A. L.; Delley, B. T. *Chem. Phys. Lett.* **2005**, *404*, 400.

(34) (a) Delley, B. *J. Chem. Phys.* **1990**, *92*, 508. (b) http://www.accelrys.com/products/materials-studio/modules/dmol3.html, accessed April 5, 2008.

(35) Perdew, J. P.; Chevary, J. A.; Vosko, S. H.; Jackson, K. A.; Pederson, M. R.; Singh, D. J.; Fiolhais, C. *Phys. Rev. B* **1992**, *46*, 6671.

(36) Perdew, J. P. *Physica B* **1991**, *172*, 1.

JP7121592